COMPUTATIONAL MECHANICS – THEORY AND PRACTICE
K.M. Mathisen, T. Kvamsdal and K.M. Okstad (Eds.)
© CIMNE, Barcelona, Spain 2003

THE EXTENDED FINITE ELEMENT METHOD FOR ARBITRARY DISCONTINUITIES

Ted Belytschko[*]
Department of Mechanical Engineering
Northwestern University
2145 Sheridan Road, Room B223
Evanston, IL 60208-3111, USA
Email:
tedbelytschko@northwestern.edu
web page:
http://tam.mech.northwestern.edu/tb/tb.html

Goangseup Zi[†], **Jingxiao Xu**[†] **and Jack Chessa**[‡]
† *Department of Mechanical Engineering*
Northwestern University
Evanston, IL 60208-3111, USA
Email: g-zi@northwestern.edu and
j-xu1@northwestern.edu

‡ *Department of Mechanical & Industrial Engineering*
101 Engineering Science Complex
The University of Texas at El Paso
500 West University Avenue
El Paso, Texas 79968-0521, USA
E-mail: jfchessa@utep.edu

Abstract. Methods which can handle moving discontinuities without remeshing are presented. They make possible simple treatments of problems such as growing cracks, fluid-structure interaction, shear bands, material interfaces and phase interfaces. Methods for approximating both discontinuities in the functions and in their gradients are described. The methods are combined with level sets, so that the discontinuities can be represented entirely in terms of nodal data. This leads to simple methods with clean data structures that can easily be incorporated in general purpose software. The applications of the methods to two phase flow problems and dynamic fracture problems are given to demonstrate the methods.

Key words: extended finite element method, moving discontinuities, level sets.

1 INTRODUCTION

The methodology for approximating discontinuities independent of the finite element mesh has been incorporated in a framework which we call the extended finite element method, XFEM. An initial form of the method is reported in Belytschko and Black (1999)[i] and Moes, Dolbow and Belytschko (1999)[ii]; the methodology has recently been

generalized in Belytschko et al (2001)[iii]. The approach is based on a local partition of unity; Chessa et al. (2003) [iv], Melenk and Babuška (1996)[v].

The discontinuous approximation is constructed in term of a level set function, i.e. an implicit definition of the surface of discontinuity. Any implicit definition of the surface can be used, but generally we employ the signed distance function defined by $\phi(\mathbf{x}) = \min_{\bar{\mathbf{x}}\in\Gamma} \|\mathbf{x} - \bar{\mathbf{x}}\|$, where Γ is the surface of discontinuity. The level set field is approximated by

$$\phi(\mathbf{x}) = \sum N_I(\mathbf{x})\,\phi_I \tag{1}$$

where $N_I(\mathbf{x})$ are finite element shape functions or other interpolants. Generally, the same shape functions are used as for the approximation of the dependent variable of the solution. However, other functions can also be employed. For example, in fluid-structure interaction, we have used moving least squares approximants. These provide smooth fits to the surface of discontinuity, which is important when sliding occurs on the surface of discontinuity. Radial basis functions are advantageous when a surface needs to be constructed from a large set of scattered data.

As a consequence of the nodal definition of the geometry of the discontinuity surface, the surface of discontinuity and everything that needs to be known about the discontinuity can be represented by nodal values. This provides great simplicity to the data structure. By contrast, in surface representations of cracks in three-dimensional problems, it is necessary to construct a surface mesh. The task of matching a three-dimensional mesh to a growing surface mesh is quite overwhelming. These new methods, by relying only on nodal values to describe the discontinuity, simplify the data and make updates of evolving surfaces more straightforward.

2 APPROXIMATION OF DISCONTINUITIES

2.1 Displacement discontinuties

We will first illustrate the approach for constructing a discontinuity in a function. Two types of enrichments are used, depending on whether the support of node I is completely bisected or only partially slit by the discontinuity. The approximation for a discontinuity which bisects the support of a finite element shape function, $N_I(\mathbf{x})$, is given by

$$\mathbf{u}(\mathbf{x},t) = \sum_{I\in\mathcal{N}} N_I(\mathbf{x})\,\mathbf{u}_I + \sum_{I\in\mathcal{N}^{enr}} N_I(\mathbf{x})\,H\big(\phi(\mathbf{x})\big)\,\mathbf{a}_I \tag{2}$$

where $\mathbf{u}_I$ are the usual nodal values of the approximation, $\phi(x)$ is the signed distance function which describes the discontinuity, $\mathcal{N}$ is the set of all nodes and $\mathcal{N}^{enr}$ is the set of enriched nodes and $H(\cdot)$ is the step function. The parameters $\mathbf{a}_I$ are called enrichment parameters; these are additional unknowns in the discrete system that enable the strength of the discontinuity to vary along its length. For purposes of efficiency, only the nodes of elements cut by the discontinuity are enriched. Note that the first part of the right hand side is a standard C^0 finite element approximation. Figure 1 shows how the elements are enriched for a typical discontinuity. An attractive feature of this approach is that the enrichment is local, so that the discrete system of equations remains sparse.

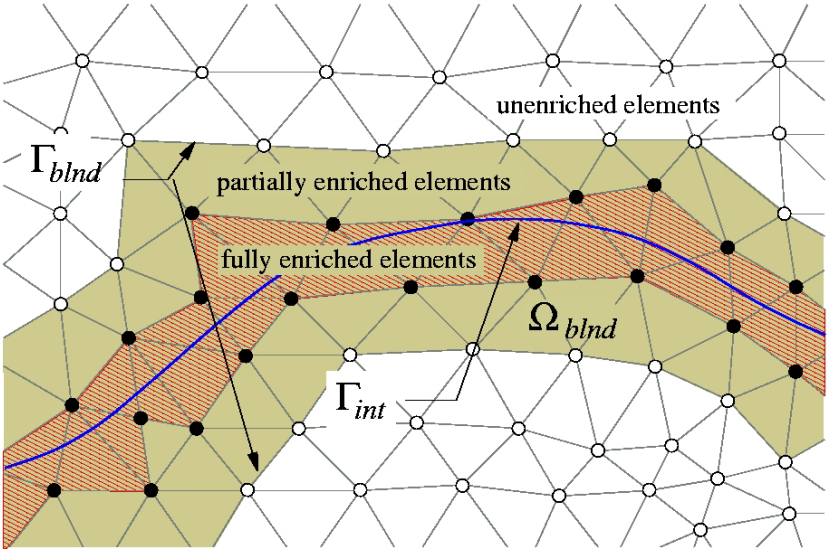


Figure 1: Local partition of unity enrichment for a typical finite element mesh with an interface, showing elements that are fully enriched, partially enriched and unenriched. Also shown is the boundary Γ_{blnd} where the enrichment vanishes

For a support which is slit by the discontinuity, the approximation is

$$\mathbf{u}(\mathbf{x}) = \sum N_I(\mathbf{x})\left(\mathbf{u}_I + \mathbf{a}_{\alpha I} b^D_{\alpha I}(\mathbf{x})\right) \tag{3}$$

where $b^D_{\alpha I}(\mathbf{x})$ can for example be given by

$$b^D_{\alpha I}(\mathbf{x}) = \left[r\cos\frac{\theta}{2},\ r^2\cos\frac{\theta}{2},\ \sqrt{r}\cos\frac{\theta}{2} \right] \tag{4}$$

The function can also be modified by subtracting its values at the nodes.

2.2 Gradient discontinuties

Another important class of discontinuities are those in the first derivatives of the approximation, i.e. the gradient. Such discontinuities occur at interfaces between different materials and different phases of materials. From a more general viewpoint, we can say that discontinuities in derivatives occur wherever the coefficients of the governing partial differential equation are discontinuous. These discontinuities can easily be handled by standard finite element approximations when the element edges coincide with the discontinuity. However, this requires the mesh generator to account for the discontinuity, which is often difficult. Furthermore, if the discontinuity moves with time, remeshing is required.

An approximation with a discontinuity in the gradient is constructed by letting the nodal approximation for a node with a bisected support be

$$\mathbf{u}(\mathbf{x},t) = \sum_{I\in N} N_I(\mathbf{x})\mathbf{u}_I + \sum_{I\in N^{enr}} N_I(\mathbf{x})\left|\phi(\mathbf{x})\right|\mathbf{a}_I \tag{5}$$

For intersecting and branching discontinuities in derivatives, the same procedure as for discontinuities in the function can be used. For example, for two intersecting discontinuities, the approximation is

$$\mathbf{u}(\mathbf{x}) = \sum N_I(\mathbf{x})\left(\mathbf{u}_I + \mathbf{a}_{I1}\left|\phi_1(\mathbf{x})\right| + \mathbf{a}_{I2}\left|\phi_2(\mathbf{x})\right| + \mathbf{a}_{I3}\left|\phi_1(\mathbf{x})\right|\left|\phi_2(\mathbf{x})\right|\right) \tag{6}$$

3 DISCRETIZATION

The discrete equations are developed from a weak form. For the case of continua, the weak form is the principle of virtual work. One of the major difficulties of the method is that the integrands in elements cut by discontinuities are also discontinuous. Therefore, the weak form in these elements cannot be integrated directly by Gauss quadrature.

We are using two methods for treating the quadrature of these elements:

1. Methods in which the elements with discontinuities are split into subelements so that the discontinuities correspond to edges of the subelements.
2. Smoothing methods in which the integrand is smoothed around the discontinuity by a regularization expressed in terms of the level set function.

XFEM is very compatible with the structure of general purpose finite element programs. It requires only nodal data, and it can be added to existing programs through an element gateway. Therefore, there is a high probability that these methods will be adopted by finite element code developers.

4 APPLICATION EXAMPLES

4.1 Two flow problems

Solutions of two-phase immiscible flow problems by a hybrid XFEM/level set method is described next. The initial method was described in Chessa and Belytschko (2003)[vi]. In this method, the fluid phase interface is tracked by a level set function. The velocity field is enriched with a function whose gradient is discontinuous across the interface. This results in a discontinuity in the rate of deformation tensor, thus improving the accuracy of the approximation at the interface without the need for remeshing. The enrichment is expressed in terms of the level set function. The level set field uses the same finite element mesh and is updated by a characteristic Galerkin method. The computational overhead of the level set update is minimized by only solving in a narrow band about the interface. We have now improved the construction of the enrichment for discontinuous gradients. This is described in Chessa et al (2003)[iv]. In addition, methods for treating surface tension have been incorporated in Chessa and Belytschko (2003)[vi]. The accuracy of the method has been demonstrated in several examples.

As an example we consider an immersed air bubble in water rising to the air-water free surface as shown in Figure 2. The results are compared to two terminal velocity formulae in Figure 3. It can be seen that the numerical solution falls between the bounds.

Figure 4 shows a bubble dropping to a thin film. Although no exact solution is available for this problem, the solution appears qualitatively reasonable. The method's ability to handle the complex topological changes in the interface is shown as bubble

deforms during its fall and impacts the film. As would be expected depending on the mesh size the resolution of fine scale features in the interface differs somewhat.

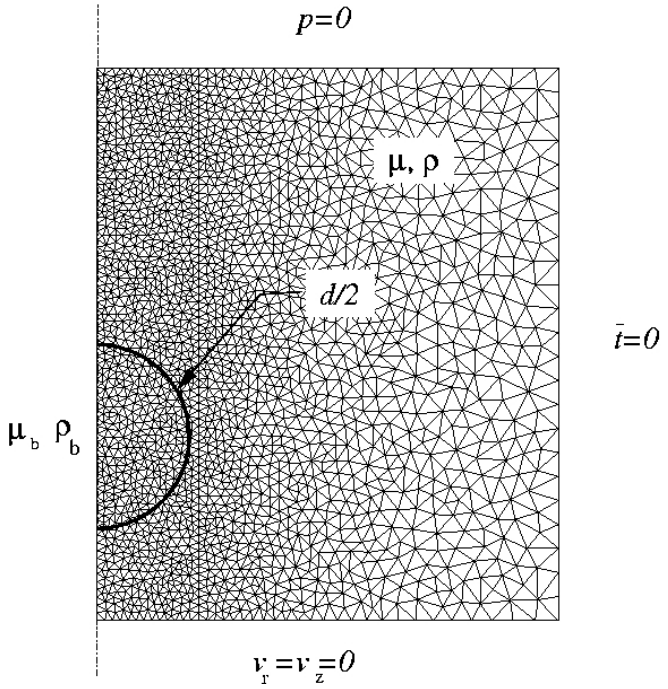


Figure 2: Computational domain for the buoyancy driven bubble.

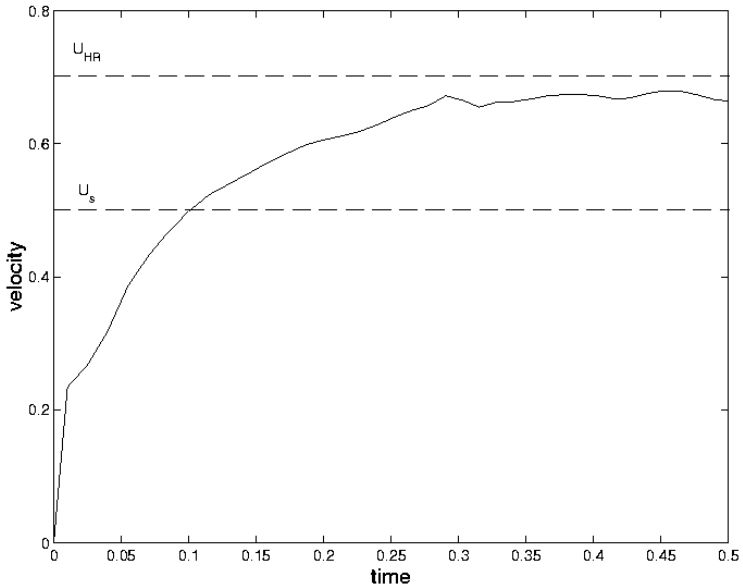


Figure 3: Plot of the velocity of the bubble centroid from the terminal velocity computation versus time. Also the Stokes and Hadamard-Rybczynski terminal velocities are shown.

Figure 5 shows two bubbles driven to the surface by buoyancy forces. The bubbles are of differing diameters but of the same constituent fluid, benzene. The bubbles rise to a free surface in a secondary fluid, water, due to buoyancy. The fluid above the free surface is benzene as well. The larger bubble has a radius of 0.750 cm and the smaller

bubble has a radius of 0.375 cm. The two bubbles will rise at different rates due to their differing buoyancy forces. The Eötvös numbers for the larger and smaller bubbles are 27.25 and 6.81, respectively; the Morton number, which is independent of the bubble dimension, is 1.77×10^{-9} for both bubbles. The problem has been run on a coarse unstructured discretization and several structured meshes, including a fine 80×154 mesh. The initial conditions for the problem are zero velocity and hydrostatic pressure, and the problem was run for a sufficient period of time so that the merging of the bubbles and their subsequent rising through the free surface can be seen.

Figure 5 also shows the velocity vectors, pressure and interface position at several time steps during the simulation. The results appears qualitatively reasonable and illustate the robustness of the method in handling such difficult topological changes of the interface.

Figure 6 shows the identical simulation with an unstructured mesh. The results are initially quite similar, but towards the end of the simulation significant differences develop. For example, the two bubbles coalesce much earlier in the simulation. It may be that an unstructured mesh destabilizes the interface easier. This is now under study.

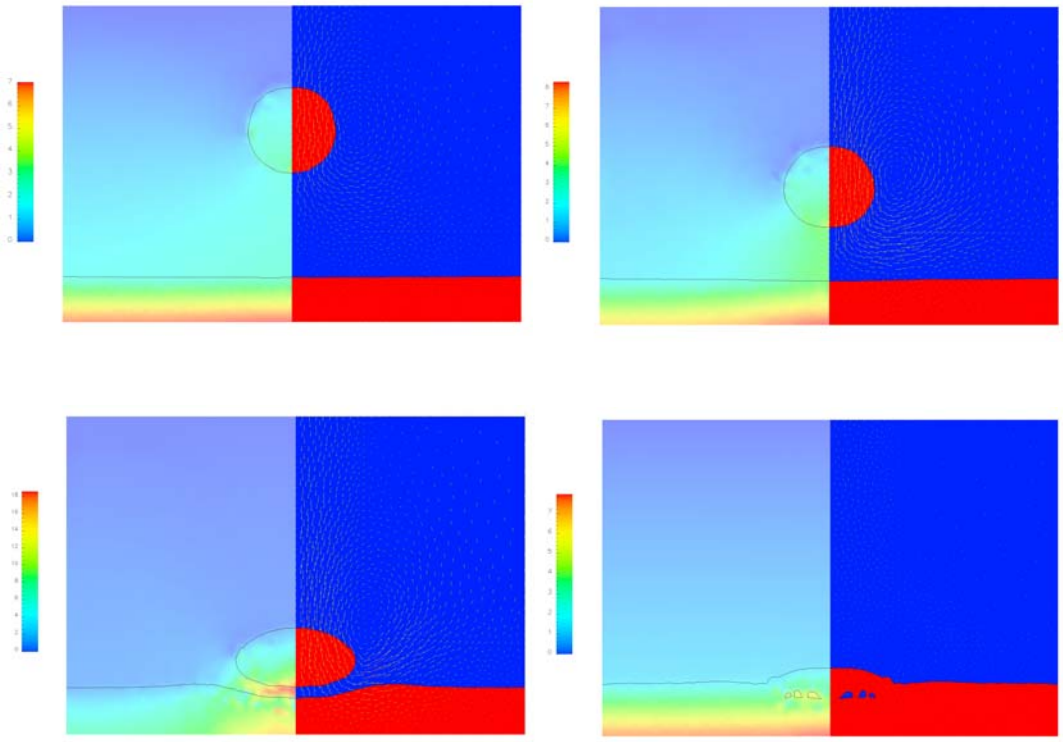


Figure 4: Numerical solution of drop falling to a thin film at four different time steps. The pressure is the plotted along the velocity vectors and the phase interfaces for mesh 1.

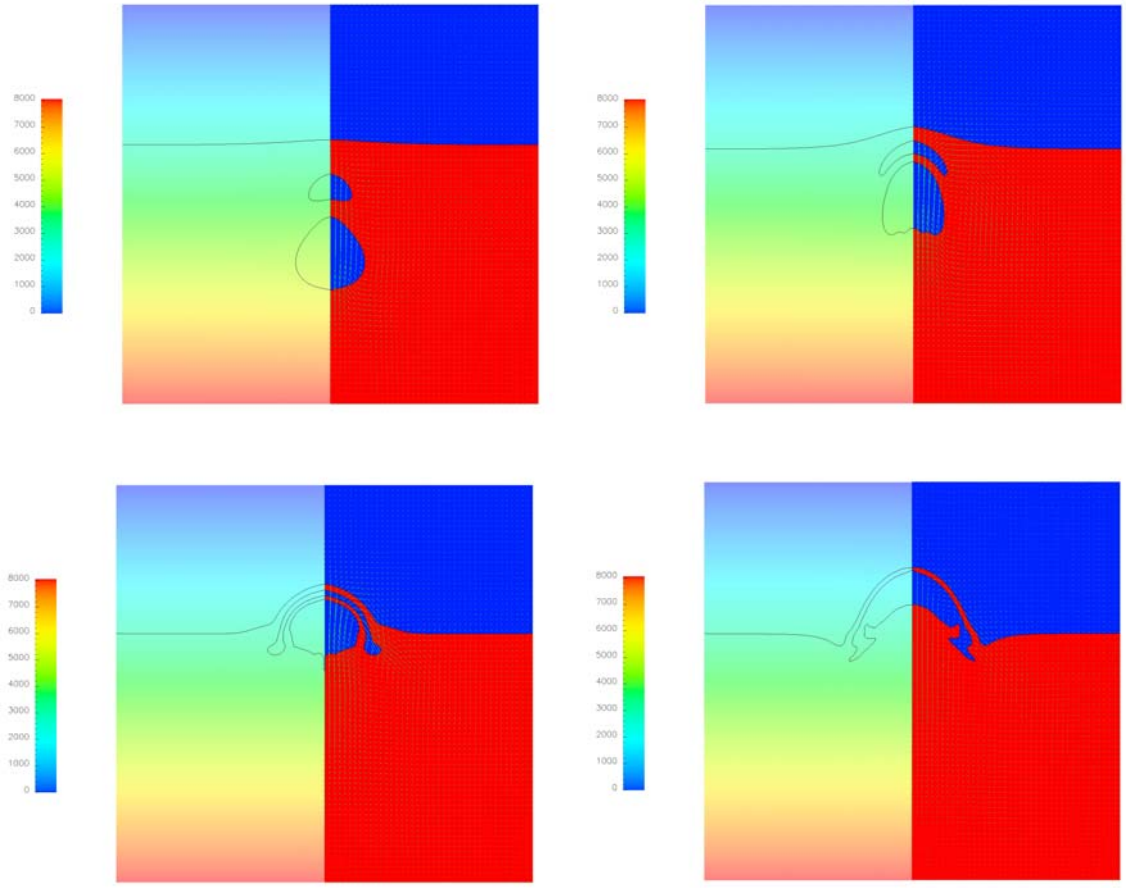


Figure 5: Numerical solution of two bubbles rising to a fluid interface surface at four different time steps for the structured grid. The Pressure is the plotted on the left hand side along the velocity vectors and the phase interfaces on the right hand side (CGS units).

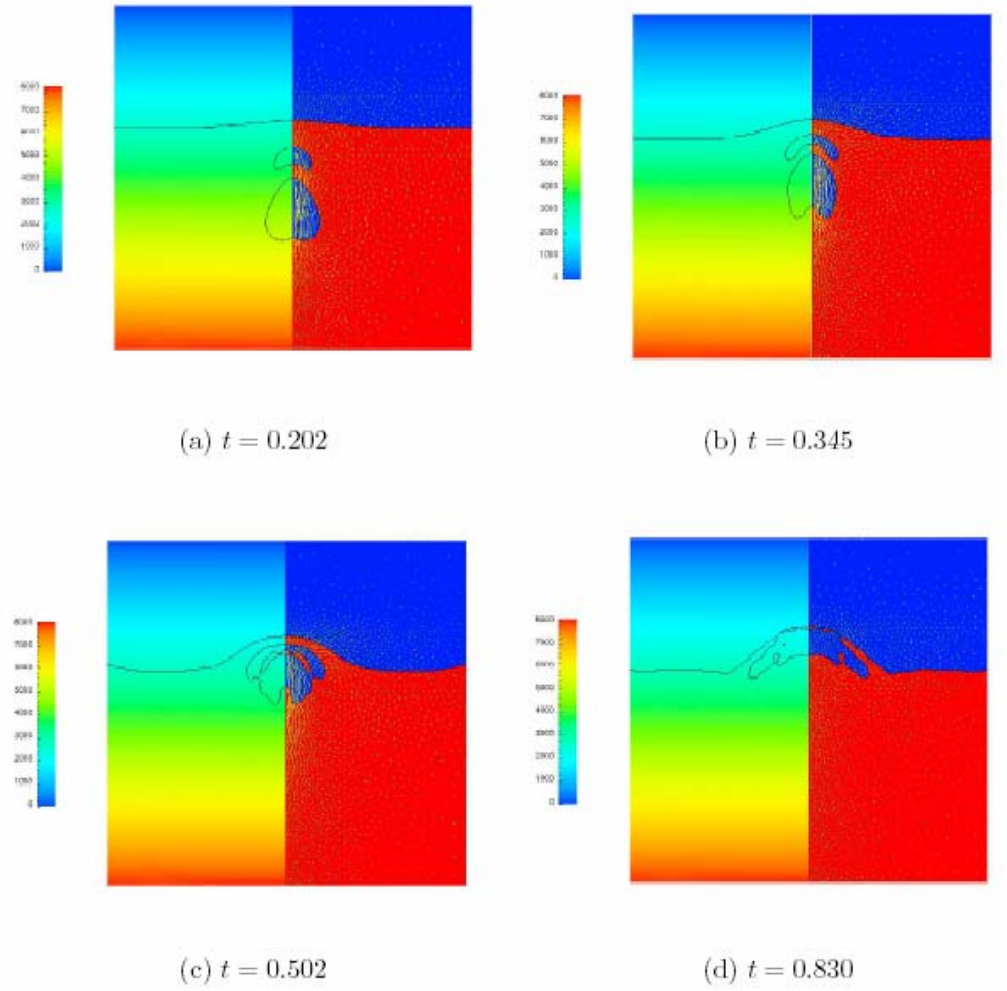


Figure 6: Numerical solution of two bubbles rising to a fluid interface surface at four different time steps for the coarse unstructured grid. The Pressure is the plotted on the left hand side along the velocity vectors and the phase interfaces on the right hand side (CGS units).

4.2 Fracture problems

A major obstacle in extending the original XFEM method[i,ii] to dynamic cracks is that in the latter, the enrichment around the crack tip is a branch function of the form $\sin(\theta/2)$, where θ is the angle to the crack tip. This enrichment function does not blend naturally to the step function enrichment that is required once the crack completely cuts the element.

Therefore a new enrichment has been developed for elements partially cut by a crack[vii]. The idea underlying these new enrichment functions is that they should naturally progress to the step function enrichment as the crack passes though the element.

The crack is driven by a loss of hyperbolicity criterion. The following describes our methodology for using the loss of hyperbolicity criterion to propagate the crack. The methodology described here is only applicable to rate-independent materials. This method also allows a new crack to initiate and determines its direction. Thus there is no need for a crack growth law: the crack growth, i.e. the cracktip velocity and the direction of the crack, are determined by the constitutive equation.

In essence, the method uses the polarization of the plane wave emanating from the hyperbolicity condition to set the direction of the crack and the value of the hyperbolicity condition to set the speed. Let

$$e = \min_{\boldsymbol{n},\boldsymbol{h}} (n_i h_j A_{ijkl} n_k h_l) \tag{7}$$

where A is the material tangent modulus. We call *e* the hyperbolicity indicator. The momentum equations remain hyperbolic as long as *e*>0. If the inequality *e*>0 is violated in the neighborhood of a cracktip, we then choose the normal of the surface increment (line increment in two dimensions) to be the vector $\boldsymbol{n}$ that minimizes *e*. The direction of the cracktip is denoted by a unit vector $\boldsymbol{s}$, and it is given by

$$\boldsymbol{s} \bullet \boldsymbol{n} = 0 \tag{8}$$

The hyperbolicity indicator is a piecewise continuous function in the finite element mesh, i.e. a C^{-1} function, since it depends on the tangent modulus and the stresses, which are C^{-1}. This prevents the smooth motion of the cracktip in an element. Therefore, we project *e* onto a C^0 field.

Since the hyperbolicity indicator should always vanish at the crack tip, it follows that at the crack tip.

$$\frac{\partial e}{\partial t} + v_i^c e_{,i} = 0 \tag{9}$$

where v_i^c is the velocity of the crack tip. The cracktip velocity can be expressed as

$$v_i^c = v^c s_i \tag{10}$$

where v^c is the crack speed and $\boldsymbol{s}$ is defined in (8). Substituting this definition into (9) gives

$$\frac{\partial e}{\partial t} + v^c s_i e_{,i} = 0 \tag{11}$$

from which we obtain

$$v^c = -(s_i e_{,i})^{-1} \frac{\partial e}{\partial t} = -(\boldsymbol{s} \bullet \nabla e)^{-1} \frac{\partial e}{\partial t} \tag{12}$$

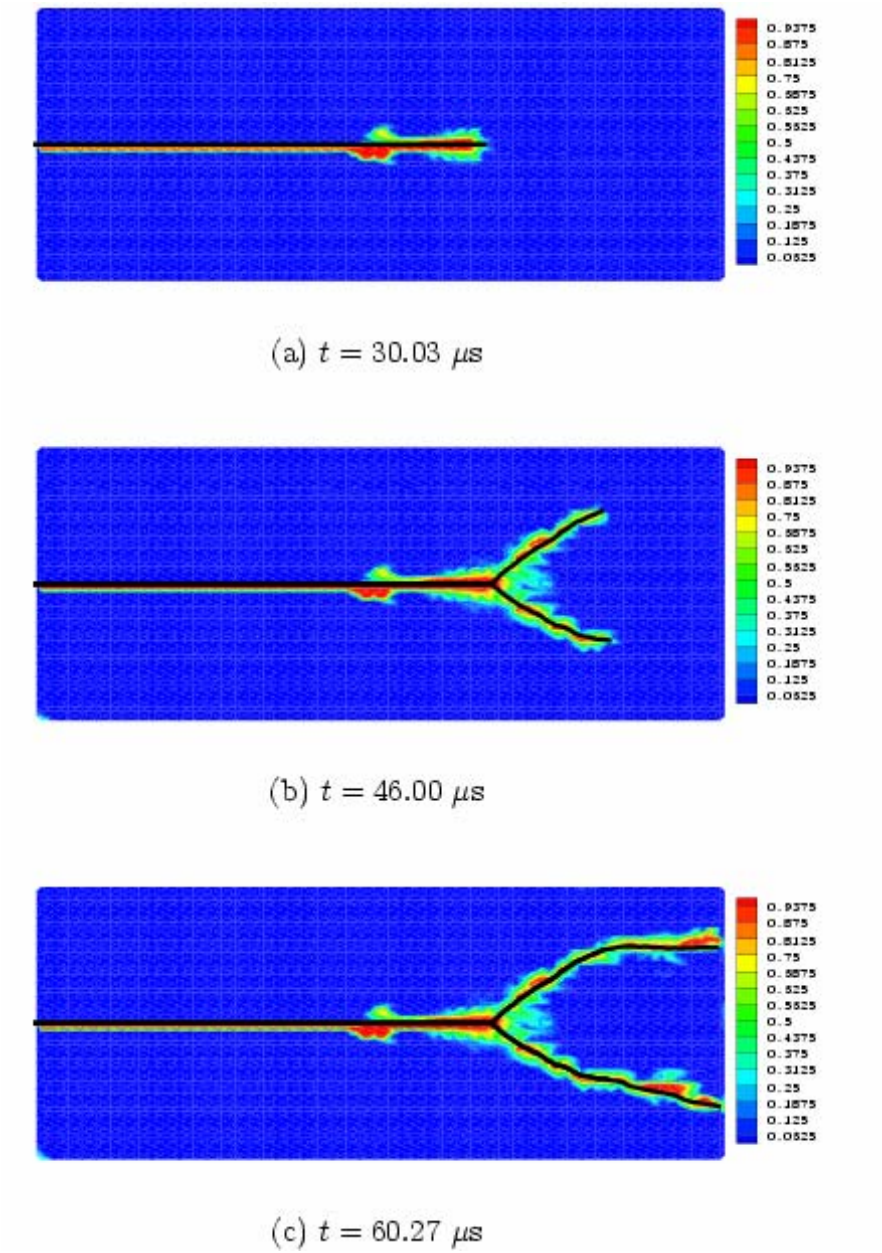
While the hyperbolicity indicator should be negative only over sets of measure zero, in numerical solutions it becomes negative in small neighborhoods around the cracktip.

An example of the propagation of a crack in a prenotched specimen by the loss of hyperbolicity criterion is given below. The rectangular specimen is of length of 0.1m and width 0.04 m. Initially a horizontal crack spans from the left edge to the center of the plate. Tensile tractions ($\sigma = 1 MPa$) are applied on the top and the bottom edges. Material constants and other parameters are given in Belytschko et al (2003)[vii].

The evolution of the crack is shown in Figure 7, and the crack speed is shown in Figure 8. The crack begins propagate at 11.34 μs and then speeds up along a straight line. During this initial phase of crack propagation, the hyperbolicity indicator at each time step is negative at the crack tip after each update of the stress field and its minimum corresponds to a vector $\boldsymbol{n}$ normal to the existing crack path. The direction of $\boldsymbol{n}$ is almost constant in the elements in the subdomain about the cracktip. The crack speed increases with time and reaches a maximum at 32.34 μs. At that point, the vectors $\boldsymbol{n}$ in elements ahead of the crack tip are no longer constant, in fact, the $\boldsymbol{n}$

vectors take on markedly different values in the elements ahead of the cracktip. We used these vectors to redirect the crack direction at this point, which resulted in branching. The ratio of the maximum crack speed (just before branching) to the dilatational wave speed is 2050/3809.5=0.54, which is significantly above the values given by Yoffe; the differences may result from difference in the material model.

After the crack branches the crack speed decreases and its velocity becomes almost constant, with a speed markedly less than the Rayleigh wave speed. Towards the end of the simulation, small branches of high damage develop around the crack. These may be secondary cracks. They are difficult to treat with our algorithm, so we have not introduced discontinuities in these small branches. The overall crack growth pattern agrees qualitatively with what has been observed in experiments. We repeated the calculation with a cross-triangular mesh of 60×25 refinement and found similar results.



(a) $t = 30.03\ \mu s$

(b) $t = 46.00\ \mu s$

(c) $t = 60.27\ \mu s$

Figure 7: Evolution of a branching crack

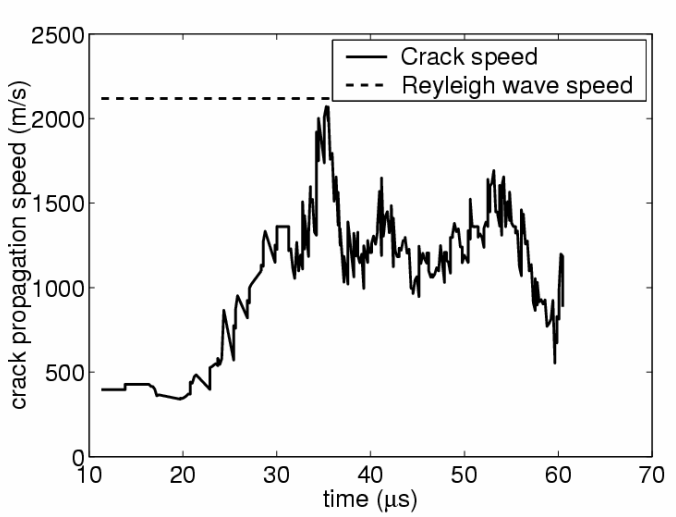


Figure 8: Crack speed for crack branching problem

A method for smoothing contact-impact surfaces that also computes the gap concurrently has been developed based on level set concepts; see Belytschko, Danniel and Ventura (2003)[iix]. Based on XFEM, a simple method for structured meshes has been formulated, see Belytschko, Xiao and Parimi (2003) [ix]. XFEM has also been extended to three dimensional problems[x-xii].

5 CONCLUSION

The extened finite element method makes simple treatments of discontinutites such as growing cracks, fluid-structure interaction, shear bands, material interfaces and phase interfaces. This method is based on the local partition of unity, which makes the enrichment local and increases computational efficiency. Examples of two phase flow and dynamic fracture demonstrated the capability of the method to handle the discontinuities.

6 REFERENCES

[1] T. Belytschko and T. Black, Elastic Crack Growth in Finite Elements with Minimal Remeshing, *Int. J. Num. Meth. Engng*, 45(5), 602-620 (1999).

[2] N. Moës, J. Dolbow and T. Belytschko, A finite element method for crack growth without remeshing, *Int. J. Num. Meth. Engng*, 46(5), 131-150 (1999).

[3] T. Belytschko, N. Moës, S. Usui, C. Parimi, Arbitrary discontinuities in finite element, *Int. J. Num. Meth. Engng*, 50, 993-1013 (2001).

[4] J. Chessa, H. Wang and T. Belytschko, On Construction of Blending Elements for Local Partition of Unity Enriched Finite Element Methods, *Int. J. Num. Meth. Engng*, 57(7), 1015-1038 (2003).

[5] J.M. Melenk, and I. Babuška, The partition of unity finite element method: Basic theory and applications, *Comp. Meth. Appl. Mech. Engng,* 39, 289-314 (1996).

[6] J. Chessa, and T. Belytschko, An Extended finite element method for two-phase fluids, *Journal of Applied Mechanics*, 70(1), 10-17 (2003).

[7] T. Belytschko, H. Chen, J. Xu, G. Zi, Dynamic Crack Propagation Based on Loss of Hyperbolicity and A New Discontinuous Enrichment, *Int. J. Num. Meth. Engng*, in press (2003).

[8] T. Belytschko T, W.J.T. Daniel, G. Ventura, A monolithic smoothing-gap algorithm for contact-impact based on the signed distance function, *Int. J. Num. Meth. Engng*, 55 (1), 101-125 (2002).

[9] T. Belytschko, S. P. Xiao, C. Parimi, Topology optimization with implicit functions and regularization, *Int. J. Num. Meth. Engng*, 57(8), 1177-1196 (2003)

[10] T. Belytschko, C. Parimi, N. Moës, N. Sukumar, S. Usui, Structured extended finite element methods for solids defined by implicit surfaces, *Int. J. Num. Meth. Engng*, 56(4), 609-635 (2003).

[11] A. Gravouil, N. Moës, and T. Belytschko, Non planar 3D crack growth by the extended finite elements and the level sets. Part II: Level set update, *Int. J. Num. Meth. Engng*,53 (11), 2569-2586 (2002).

[12] N. Moës, A. Gravouil and T. Belytschko, Non planar 3D crack growth by the extended finite elements and the level sets. Part I: Mechanical Model, *Int. J. Num. Meth. Engng*, 53 (11), 2549-2568 (2002).